Comprehensive research on self phase modulation based optical delay systems*

Yang Ai-Ying(杨爱英)† and Sun Yu-Nan(孙雨南)

School of Optoelectronics, Beijing Institute of Technology, Beijing 100081, *China*

(Received 22 March 2010; revised manuscript received 13 May 2010)

This paper comprehensively investigates the properties of self phase modulation based optical delay systems consisting of dispersion compensation fibre and highly nonlinear fibres. It researches into the impacts of power level launched into highly nonlinear fibres, conversion wavelength, dispersion slope, modulation format and optical filter bandwidth on the overall performance of optical delay systems. The results reveal that, if the power launched into highly nonlinear fibres is fixed, the time delay generally varies linearly with the conversion wavelength, but jumps intermittently at some conversion wavelengths. However, the time delay varies semi-periodically with the power launched into highly nonlinear fibres. The dispersion slope of highly nonlinear fibres has significant influence on the time delay, especially for the negative dispersion slope. The time delay differs with modulation formats due to the different combined interaction of nonlinearity and dispersion in fibres. The bandwidth of the optical filters also greatly affects the time delay because it determines the bandwidth of the passed signal in the self phase modulation based time delay systems. The output signal quality of the overall time delay systems depends on the conversion wavelength and input power level. The optimisation of the power level and conversion wavelength to provide the best output signal quality is made at the end of this paper.

Keywords: optical fibre delay, fibre optics, self phase modulation, optical fibre dispersion

PACC: 4230Q, 4265K, 4280S, 4281D

1. Introduction

Optical delay systems have many applications in different areas including buffering and delaying signals during their processing in the nodes of an optical network, optical signal processing and optical control of phased array antennas in microwave communications.[1] Up to date, different approaches have been demonstrated to realize optically controllable delay, such as the recirculation of light in a ring resonator and the switching of light between different optical paths in a lightwave circuit can be used to achieve discretely tunable optical delay.[2,3] Alternatively, continuous optical delays have been demonstrated by using parametric amplifiers and a dispersive fibre,[4] slow-light based techniques,[5−8] resonant optical filters,[9] or all optical wavelength conversion involved schemes followed by signal propagation in a dispersive medium.[10−13] These schemes exhibit different characteristics in terms of the maximum delay, the delay continuity, the pulse shape degradation and the compactness. Among the all optical wavelength conversion involved schemes, the self phase modulation (SPM) based wavelength conversion is an attractive candidate because of the significant reduction of complexity and the advantage of reducing the noise that arises in data transmission.

In this paper, to the authors' knowledge, we first comprehensively investigate the properties of the continuously tunable optical delay achieved via SPM-based wavelength conversion in a highly nonlinear fibre followed by highly dispersive fibre. We research into the impacts of the power level launched into highly nonlinear fibres (HNLFs), the conversion wavelength, the dispersion slope, the modulation format, and the filter bandwidth on the overall performance, thereafter reveal the limits of such system. The simulation in this paper is carried by means of the commercial software VPItranmissionMaker 7.1.

2. Operation principle

Figure 1 is the SPM-based optical delay system studied in this paper.[14] It consists of three stages:

*Project supported by the National Natural Science Foundation of China (Grant No. 60978007) and Open Fund of Key Laboratory of Optical Communication and Lightwave Technologies (Beijing University of Posts and Telecommunications), Ministry of Education, China.

†Corresponding author. E-mail: yangaiying@bit.edu.cn

© 2010 Chinese Physics Society and IOP Publishing Ltd

wavelength conversion, dispersive delay, and wavelength re-conversion. At the wavelength conversion stage, the optical signal centred at λ_s is amplified by an Erbium-doped fibre amplifier (EDFA), filtered by the 1st optical band-pass filter (OBPF-1) and launched into the first span of HNLF1, where the optical spectrum is broadened by the SPM. Then the 2nd optical band-pass filter (OBPF-2) centred at λ_c is used to select the desired conversion wavelength window. Following the wavelength conversion stage, the converted signal propagates through the dispersion compensation fibre (DCF) and the optical delay is generated, which is proportional to the product of chromatic dispersion of DCF and conversion wavelength shift, i.e. $\Delta\tau \propto D \cdot \Delta\lambda$. Here D is the dispersion coefficient of the DCF and $\Delta\lambda$ is the conversion wavelength offset, i.e. $\Delta\lambda = \lambda_c - \lambda_s$. After the dispersive delay stages, the delayed signal is amplified by another EDFA and launched into the second span of HNLF2. The optical spectrum is broadened again, and the 3rd optical band-pass filter (OBPF-3) centred at λ_s is used to make the delayed output signal have the same wavelength as the original input signal. The variable optical attenuators (VOAs) in the system are used to control the power launched into HNLFs.

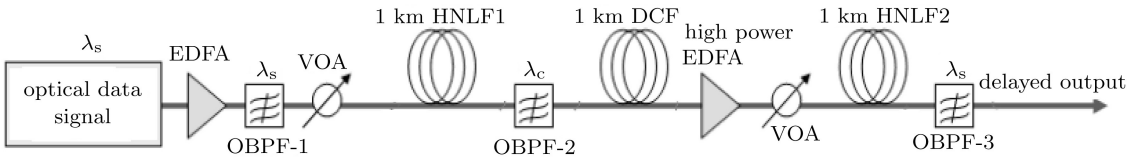


Fig. 1. Optical delay system setup. VOA: variable optical attenuator; OBPF: optical band-pass filter; HNLF: highly nonlinear fibre.

The time delay of the overall system is measured by comparing the temporal position of the output signal through tuning the centre wavelength of OBPF-2.[11,12,14] first, by tuning the central wavelength of OBPF-2 to λ_s and adjusting VOAs for no SPM broadening and the temporal position of the output signal is marked down as τ_0. Then, by increasing power levels launched into the HNLFs for exciting the SPM and tuning the central wavelength of OBPF-2 to λ_c for different optical delay, the temporal position of the output signal is marked down as τ_1. The difference between τ_0 and τ_1, i.e. $\Delta\tau = \tau_1 - \tau_0$ is defined as the time delay of the overall system with conversion wavelength of λ_c.

3. Conversion wavelength dependence of the time delay and output pulse

At the first stage of the optical delay system, the available conversion wavelength is determined by the SPM-broadened optical spectrum and whose part of the broadened spectrum is filtered out. In order to compare with the reported experimental results, the parameters used in this part are the same as that in the experiment reported by Ref. [14], i.e. the central wavelength of the original optical signal is 1545.4 nm, the nonlinear coefficient of 1 km HNLF1 is 10.9 /(W · km), the dispersion coefficient of 1 km DCF is −67 ps/(nm · km) at 1545.0 nm, and the bandwidth of OBPFs is 0.4 nm.

For the simplicity to investigate the time delay, in this part we consider a single pulse as that exploited in Ref. [12]. It is well known that the SPM-broadened spectrum can be approximately estimated by $\Delta f_{\rm SPM} \sim \Delta f_0 \gamma P_0 L_{\rm eff}$, where Δf_0 and P_0 are spectral width and peak power of the input pulse respectively, γ and $L_{\rm eff}$ are the nonlinear coefficient and effective length of HNLFs respectively. The power level launched into HNLF1 and HNLF2 can therefore be characterized by the peak power represented by P_1 and P_2. As described in Ref. [15], the SPM-broadened spectrum is accompanied by an oscillatory structure, which consists of many peak and valley points and the outermost peaks are the most intense. It may be intuitive to deduce that the conversion wavelength λ_c at peak points of the SPM-broadened spectrum is pre-

ferred and λ_c at the valley points should be avoided. But our deliberate measurements indicate that it is not the case.

We assume that the input pulse is a Gaussian pulse with full-width at half maximum (FWHM) of 25 ps. If the peak power launched into HNLFs is 35 dBm, Fig. 2(a) is the optical spectrum broadened by SPM in HNLF1. The hollow and filled circles show the peaks and valleys at the oscillatory spectrum respectively. Figure 2(b) is the filtered spectra by OBPF2 with central wavelength located at the peaks in Fig. 2(a), and Fig. 2(c) shows the corresponding time delay, which varies linearly with the conversion wavelength offset. Figure 2(d) is the output pulse of the optical delay system if the conversion wavelength locates at the respective peak point in Fig. 2(a). We notice that the output pulse is compressed at some conversion wavelengths, but is seriously distorted at other conversion wavelengths. The similar phenomenon also occurs if the conversion wavelength locates at the bottom points. The output pulse of the optical delay system is therefore conversion wavelength dependent, and the conversion wavelength at the peaks of SPM-broadened spectrum is not always the advisable choice.

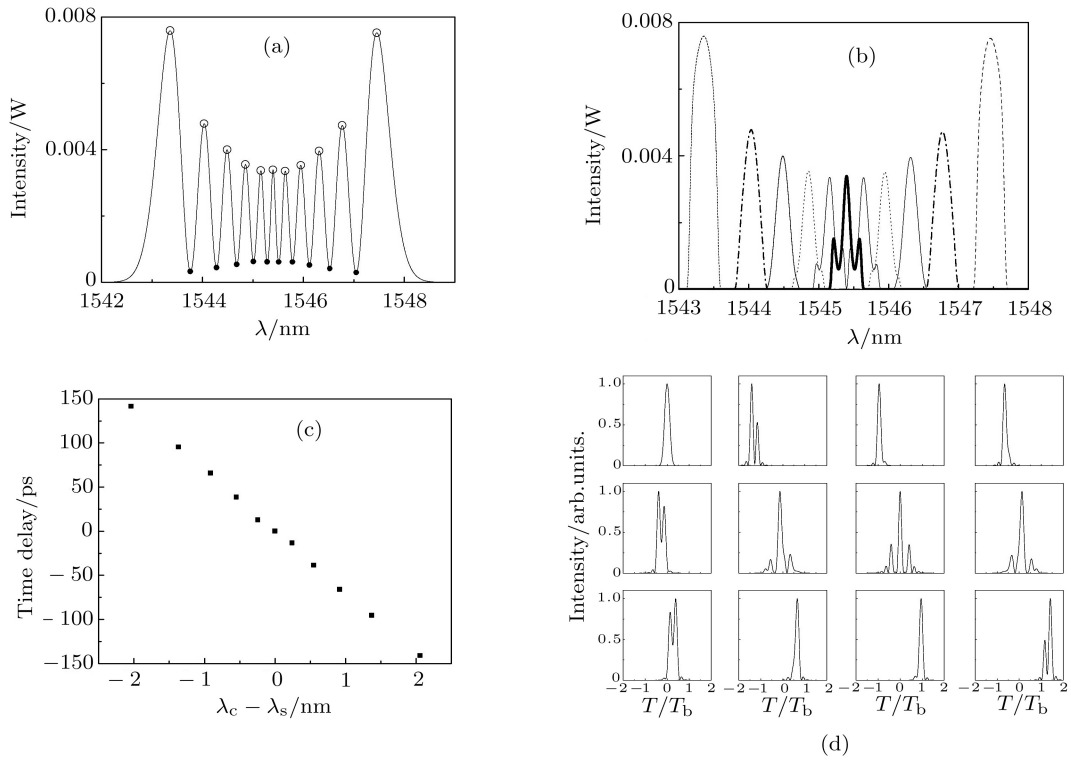


Fig. 2. Conversion wavelength dependence of the time delay and output pulse. (a) SPM broadened spectrum in HNLF1; (b) spectrum filtered by OBPF2 centred at respective peak points; (c) time delay varies linearly with the conversion wavelength shift; (d) output pulse of the overall system with different conversion wavelength, $T_b = 100$ ps.

In principle, the time delay of the overall system is proportional to the conversion wavelength shift $\lambda_c - \lambda_s$. If we change the conversion wavelength every 0.1 nm, Fig. 3(a) shows that the time delay generally varies linearly with the conversion wavelength offset as that reported for such system.[11,12,14] But the abrupt jump of time delay is also observed. The similar phenomenon exists even if the power level launched into HNLF1 and HNLF2 changes.

For example, with peak power of 33.0 and 35.0 dBm input to HNLF1 and HNLF2 respectively, the time delay jumps if the conversion wavelength offset is ±0.9 nm. It is explained by the output pulse shown in Fig. 3(b) that, the peak position of the seriously distorted pulse is not at the centre of the pulse, the time delay measured by comparing the tempo-

ral position of the output pulse peak therefore jumps. The reason for the seriously distorted output pulse is inherently attributed to complicated interaction of the intra-channel dispersion and nonlinearity.

It can be concluded from the above discussion that the output pulse and time delay depend on conversion wavelength. The time delay jumps at some conversion wavelengths, and serious distortion correspondingly occurs to the output pulse of the overall system. The distorted pulse implies the degraded signal quality. It is therefore indispensable to evaluate the output signal quality together with the time delay for an optical delay system.

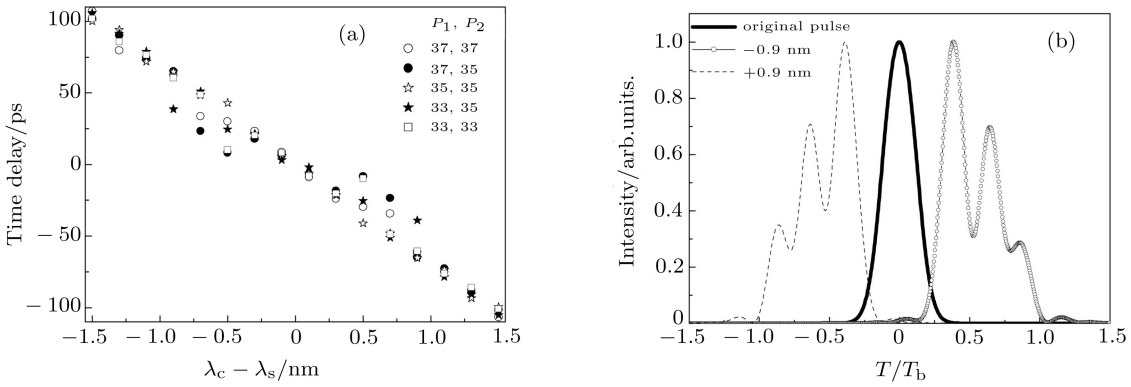


Fig. 3. Conversion wavelength dependence of time delay system. (a) time delay; (b) output pulse.

4. Power dependence of time delay and output pulse

It is noticed in Fig. 3(a) that, for different sets of power level launched into HNLFs, the slope of the time delay is almost the same except that the time jumps at different conversion wavelength.

The power dependence is therefore studied with a given conversion wavelength in this part. The given conversion wavelength is 1544.4 nm, i.e. −1.0 nm conversion wavelength offset from the original signal. For the simplicity of analysis, the dispersion of HNLFs and the nonlinearity of DCF are ideally neglected.

First, we change the peak power P_2 launched into HNLF2 and fix the peak power P_1 launched into HNLF1. Figures 4(a) and 4(b) show the semi-periodic variation of time delay and power intensity at the given conversion wavelength after HNLF2. The varying direction of time delay is almost opposite to the power intensity. It can be simply explained by the interaction of inter-channel chirp induced by SPM in HNLFs and chromatic dispersion in DCF. If the peak power launched into HNLF1 is fixed to 35 dBm, Fig. 5 shows that the output pulse of the overall optical delay system changes with the peak power launched into HNLF2. It is observed that, the pulse is compressed if the peak power launched into HNLF2 is 36.2, 31.0, 33.1, 34.4 dBm respectively, which corresponds to the intensity peak in Fig. 4(b), therefore the time delay system has the reshaping function. But the pulse is split if the power corresponds to the intensity bottom in Fig. 4(b), meaning that the output pulse is seriously distorted. It is therefore concluded that, the power launched into HNLF2 has great impact on the time delay and the output pulse. The former is due to the inter-channel interaction between chromatic dispersion and nonlinearity, and the latter is due to the intra-channel interaction between the two factors.

Then, we change the peak power P_1 launched into HNLF1 and fix the peak power P_2 launched into HNLF2. Figures 4(c) and 4(d) show the similar variation of time delay as that in Figs. 4(a) and 4(b), but the intermittent jump of time delay occurs around the bottom part of the power intensity curve. To change the given values of P_2, the jump of time delay happens at different values of P_1. Finally, we set that the peak power launched into HNLF1 and HNLF2 are same. Figure 6 shows that the variation of time delay is similar to that in Fig. 4.

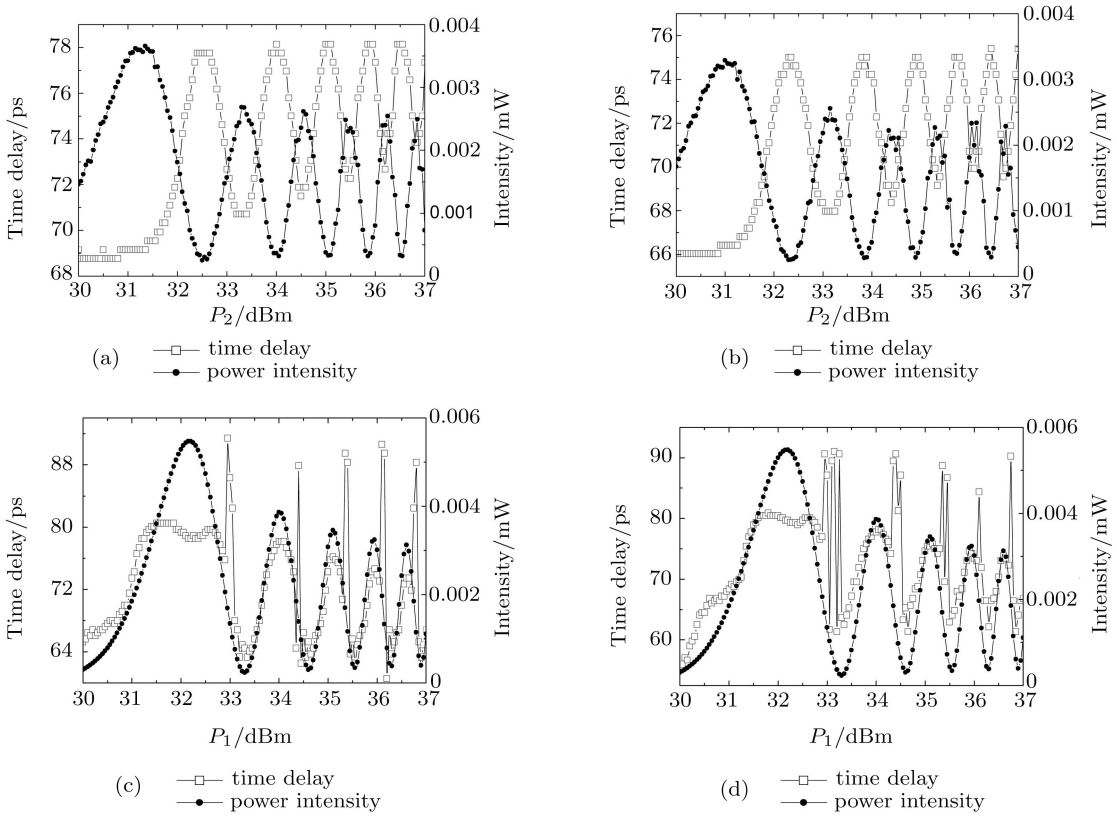


Fig. 4. Time delay changes with peak power launched into HNLF2. (a) $P_1 = 34$ dBm; (b) $P_1 = 35$ dBm. Time delay changes with power launched into HNLF1: (c) $P_2 = 34$ dBm; (d) $P_2 = 35$ dBm.

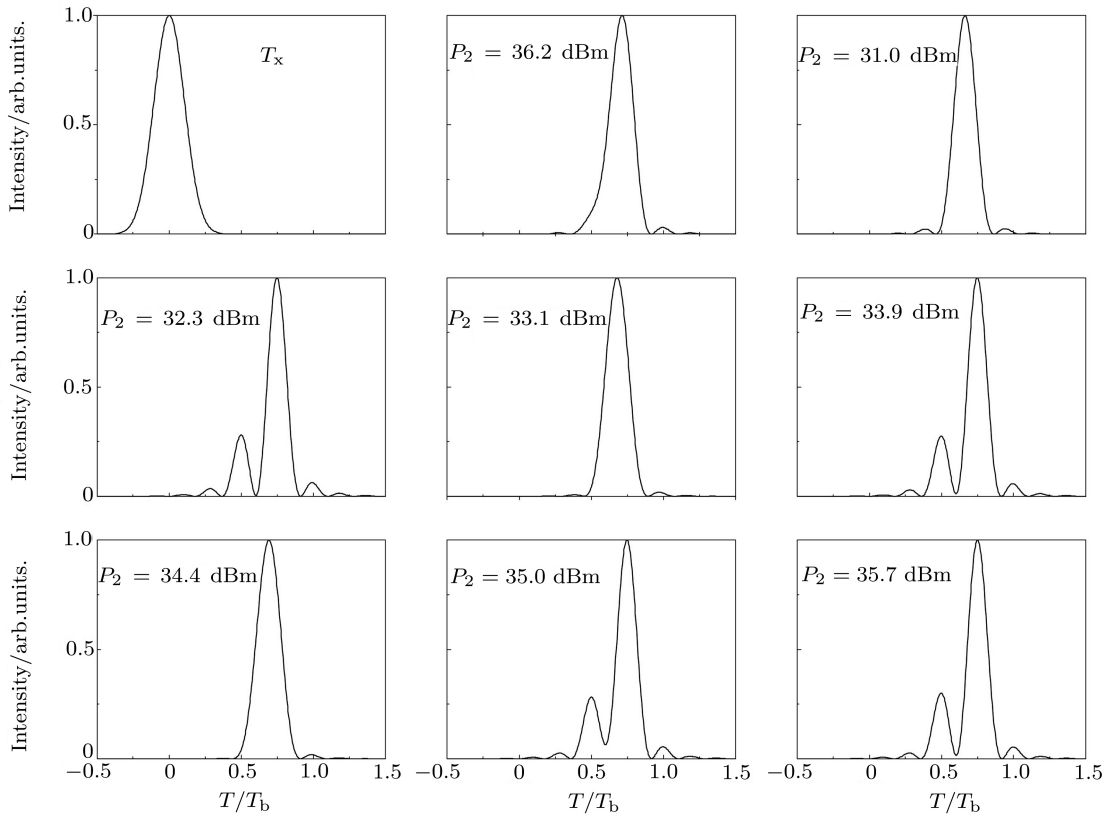


Fig. 5. Output pulse changes with power launched into HNLF2. Power launched into HNLF1 is fixed to 35 dBm.

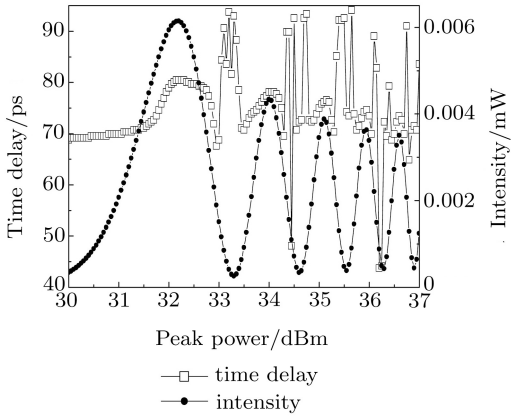


Fig. 6. Time delay changes with the power launched into HNLFs. The given conversion wavelength is 1544.4 nm.

The results in Figs. 4–6 are obtained without considering the chromatic dispersion in HNLFs and nonlinearity in DCF. Now we consider the chromatic dispersion in HNLFs and nonlinearity in DCF. Figures 7(a) and 7(b) show the time delay changes with the power launched into HNLFs, where the conversion wavelength is 1544.4 nm and 1544.6 nm respectively. Similar to Fig. 6, the time delay also jump around the bottom part of the intensity curve. But if plot the results of Figs. 6 and 7(a) in Fig. 7(c), we can see that, in a variation period, the time delay decreases slightly at first before it begins to increase, meaning that the nonlinearity in DCF and chromatic dispersion in HNLFs also affects the time delay. Figure 7(d) is the output pulse with different power launched into HNLFs, and the given conversion wavelength is 1544.6 nm. Referred to time delay in Fig. 7(b), it can be found that the output pulse with the jumped delay is seriously deformed. For example, the time delay jumps if peak power launched into HNLFs is 35.0 dBm, and the corresponding output pulse is seriously distorted. It means that where the time delay jumps, the corresponding output pulse is seriously deformed.

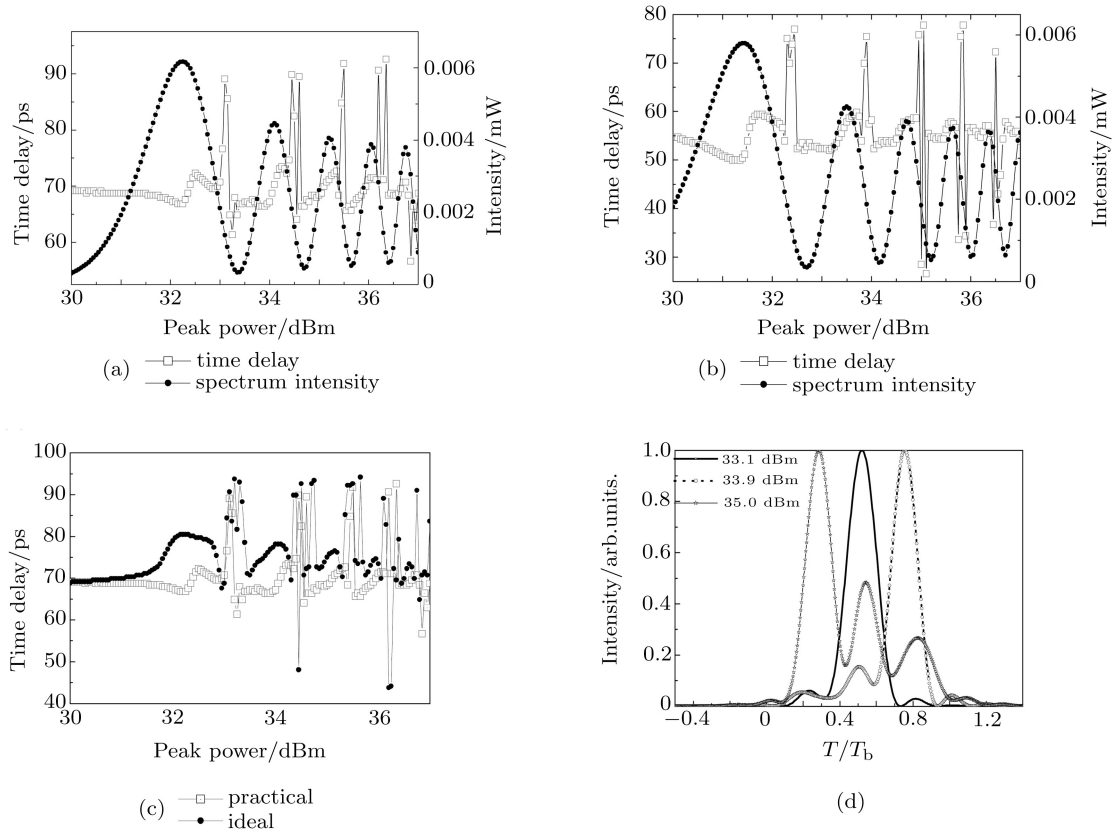


Fig. 7. Power dependence of an optical delay system. (a) Time delay and spectrum intensity for the conversion wavelength at 1544.4 nm and (b) 1544.6 nm. (c) Comparison of time delay under ideal and practical condition. (d) Output pulse of overall optical delay system.

It can be concluded from the above discussions that the output pulse and time delay depend on power level. The varying direction of time delay is generally opposite to that of the intensity at the conversion wavelength. But intermittent jump of time delay occurs due to the complicated impact of power launched into HNLF1. It is therefore concluded that, in order to obtain the required time delay, the power launched into HNLF1 and HNLF2 needs to be deliberately chosen, which therefore limits the convenience of the SPM-based time delay system.

5. Impact of dispersion slope on the time delay

It is well known from Ref. [15] that, the impact of dispersion slope should be considered if the operation wavelength is near the zero dispersion point. It can therefore be predicted that, the dispersion slope in HNLF should be considered, and can be negligible in DCF. In this part, we simulated the time delay when the dispersion slope is considered. The simulated results verify that the dispersion slope of DCF has negligible impact on the time delay. But the impact of dispersion slope in HNLFs can not be neglected if the conversion wavelength is not far from the zero dispersion wavelength of HNLF. To set that the zero-dispersion wavelength of HNLFs is 1557 nm, Fig. 8 shows that the impact of the dispersion slope is significant if the dispersion slope is -0.1 ps/(km $\cdot$ nm^2), and the influence on time delay is greater for negative dispersion slope. As a result, the time delay jumps greatly at some conversion wavelengths.

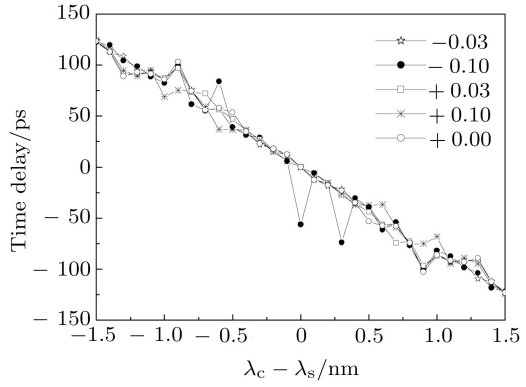


Fig. 8. Influence of dispersion slope on time delay. The zero-dispersion wavelength of HNLFs is 1557 nm.

6. Impact of different duty-cycle modulation formats on time delay

Because the spectrum of different modulation format signal is different, it is not hard to understand that the SPM-broadened spectrum is dependent on the modulation format. Figure 9 shows that, with

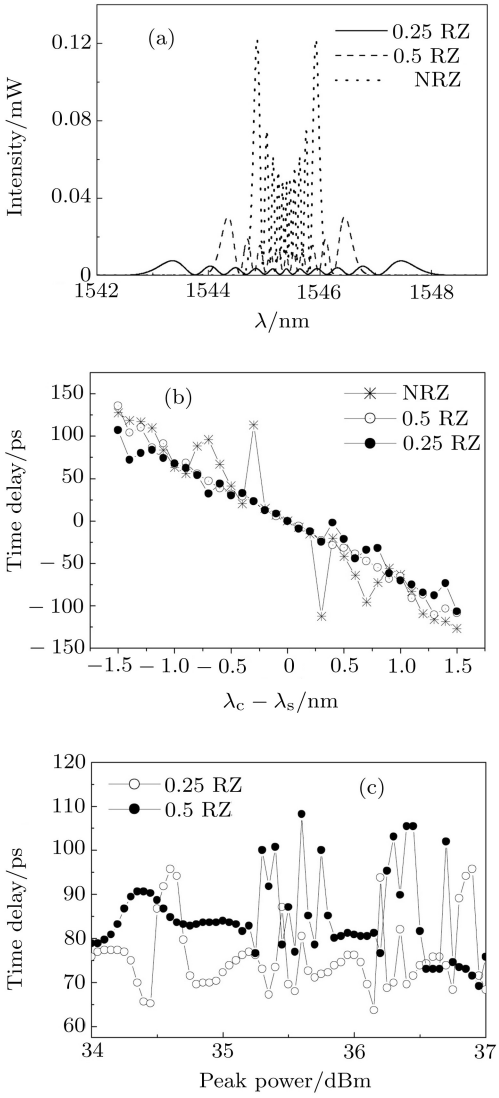


Fig. 9. (a) The SPM broadened spectra for different modulation formats. (b) and (c) Time delays for different modulation formats.

the same peak power, the optical spectrum is more widely broadened for the return-to-zero (RZ) signal with smaller duty cycle. The time delay is determined by the available conversion wavelength, which depends on bandwidth of the SPM-broadened spectrum. It is therefore deduced that the available time delay depends on modulation format. For example, in Fig. 9(a), the available conversion wavelength is

1543∼1548 nm for 0.25 RZ signal, but the conversion wavelength is limited to 1544.6∼1546.4 nm for non-return-to-zero (NRZ) signal. Figures 9(b) and 9(c) are the time delays for different modulation formats. In Fig. 9(b), the peak power launched into HNLFs is 37 dBm, and bandwidth of the OBPFs is 0.4 nm. The jump of time delay differs with different modulation formats. In Fig. 9(c), the conversion wavelength is 1544.4 nm, and the powers launched into HNLF1 and HNLF2 are the same. The difference of time delay is explained by the fact that the combined impacts of the intra-channel nonlinearity and chromatic dispersion are different for various duty cycle modulation format signal.

7. Impact of OBPFs' bandwidth on time delay

In order to study the impact of the bandwidth of OBPFs on the optical delay system, we first tune the VOAs in Fig. 1 to make power launched into HNLFS for no significant SPM and tune the central wavelength of OBPF-2 the same as the original signal. For 0.5 RZ format signal, the output pulse will be almost the same as the original pulse when the bandwidth OBPFs is greater than $3R_{\rm b}$, where $R_{\rm b}$ is the bit rate of the signal. However, when higher power is launched into HNLFs and the SPM excited, the time delay of optical delay system will be greatly influenced by the bandwidth of the OBPFs. Given that the peak power launched into HNLFs is 35 dBm, Fig. 10(a) shows that the time delay is significantly different for optical delay systems with the optical filters bandwidth of $3R_{\rm b}$ and $8R_{\rm b}$. The optical filters determine the bandwidth of the passed signal, so the bandwidth closely-dependent intra-channel nonlinearity and chromatic dispersion are greatly affected. As a result, the output waveform and time delay vary with the optical filter bandwidth. In Fig. 10(b), the conversion wavelength is fixed to 1544.4 nm, and the change of time delay with peak power launched into HNLFs also indicates the dependence of filters' bandwidth. But from the view of maintaining the waveform of the delayed signal, we prefer that the bandwidth of the OBPF is slightly wider than the original input signal.

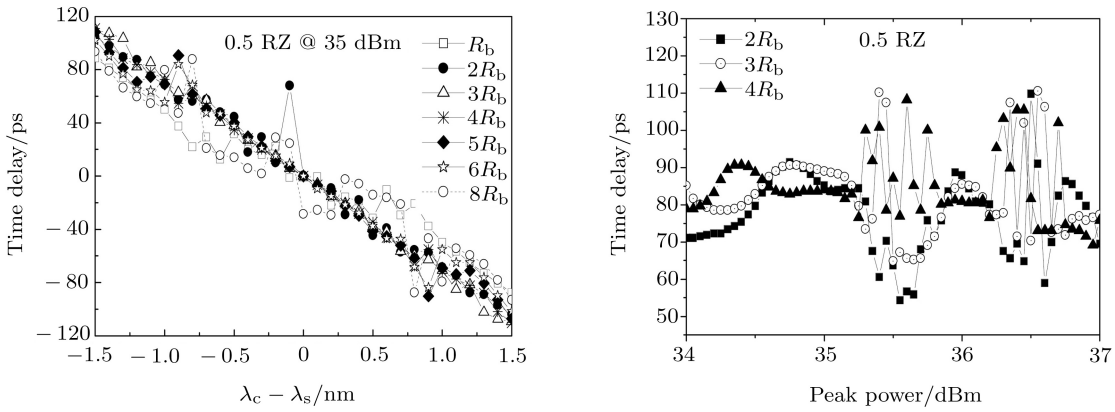


Fig. 10. Bandwidth dependence of an optical delay system. (a) The peak power launched into HNLFs is fixed to 35 dBm. (b) The conversion wavelength is fixed to 1544.4 nm.

8. Conversion wavelength and power dependence of output signal quality of SPM-based optical delay system

In this part, a 10 Gbit/s 2^8 PRBS OOK data sequence is simulated. The Q factor and eye-diagram of the output signal of the overall optical delay system are discussed. The Q factor is commonly defined as

$$Q = \frac{u_1 - u_0}{\sigma_1 + \sigma_0}, \tag{1}$$

where u_1, u_0 are the average values for "1" and "0" bits respectively, and σ_1, σ_0 are the standard deviation values for "1" and "0" bits. In this paper, we express Q in dB as

$$Q(\mathrm{dB}) = 20\lg Q. \tag{2}$$

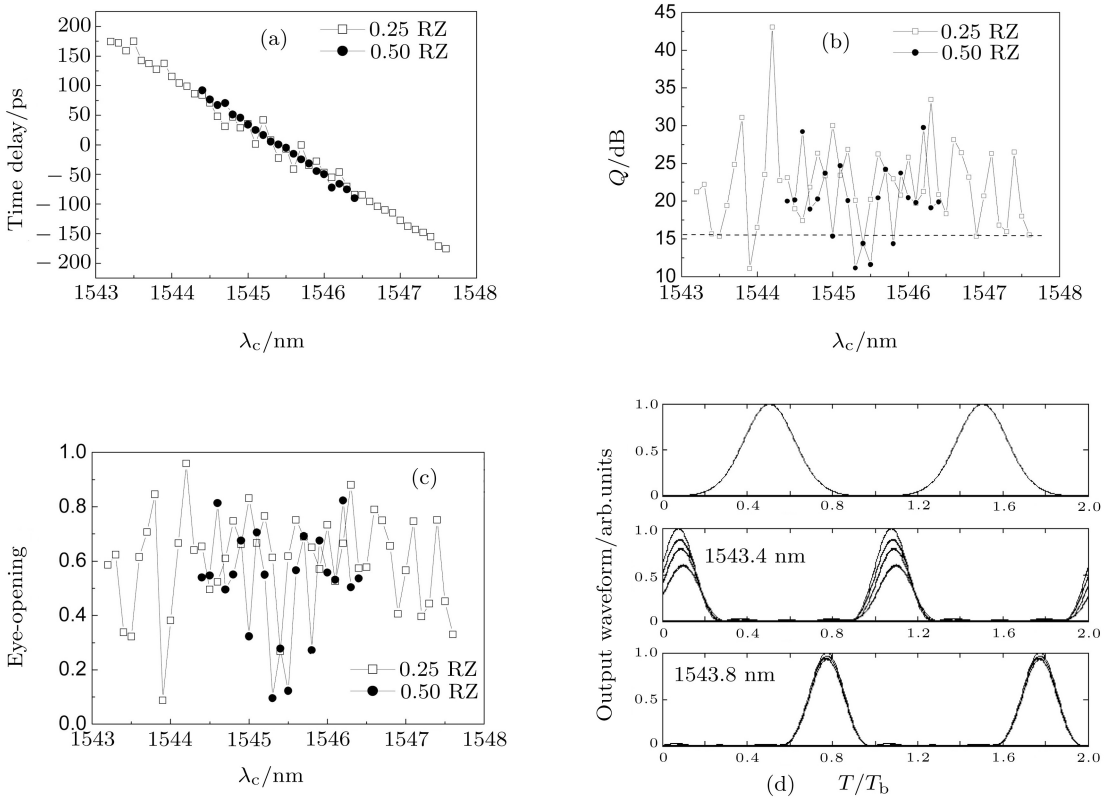


Fig. 11. Conversion wavelength dependence of optical time delay system. (a) time delay; (b) Q factor; (c) eye-opening; (d) output waveform. The dashed line in (b) indicates the required Q factor corresponding to BER of 10^{-9}.

The average power of the original optical signal is 0.0 dBm and is amplified by an EDFA. The dispersion of DCF is -80 ps/(km · nm), the dispersion slope of HNLFs is 0.08 ps/(km · nm^2), and the other parameters of the HNLF are the same as those in Part 3. At the receiver end, we set the optical signal to noise ratio (OSNR) to be 30 dB. Considering the practically available EDFA, we assume that the average power launched into HNLF1 and HNLF2 is 27 dBm.

Figure 11(a) compares the time delay for 0.5 RZ and 0.25 RZ format signal. It is observed that the available conversion wavelength is different for the two modulation formats, and the conversion wavelength where the time delay jumps is also different. Figures 11(b) and 11(c) show the variation of Q factor and eye-opening with the conversion wavelength. In Fig. 11(b), the dashed line indicates the required Q factor corresponding to bit erro ratio (BER) of 10^{-9}. We can see that the output signal quality depends on conversion wavelength for both 0.5 RZ and 0.25 RZ signal. At some conversion wavelength, Q factor or eye-opening are greater, meaning the better output signal quality. As the example, Fig. 11(d) compares the output eye-diagram for 0.25 RZ signal of the optical delay system. The top figure is output eye-diagram for the system without optical delay by tuning the power launched into HNLFs for no significant SPM excited. The Q factor for the middle eye-diagram with the conversion wavelength of 1543.4 nm is 15.3 dB, and 31.1 dB for the bottom eye-diagrams with the conversion wavelength of 1543.8 nm respectively. The similar phenomenon occurs even if the power launched into HNLFs changes. It implies that, with the given power launched into HNLFs, there ex-

ists optimum conversion wavelength by which the output signal quality is better.

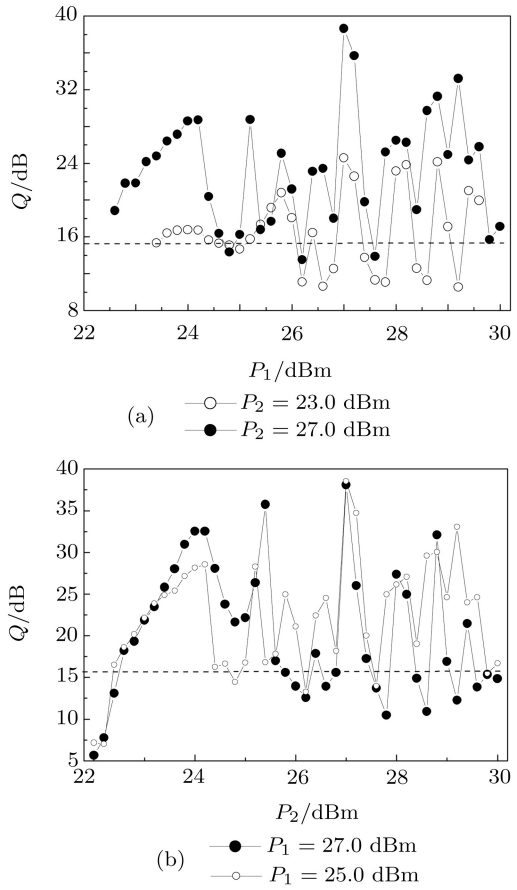


Fig. 12. Power dependence of output signal quality: (a) Q factor varies with P_1; (b) Q factor varies with P_2. The dashed line indicates the required Q factor corresponding to BER of 10^{-9}.

Then the power dependence of output signal quality is studied for 0.25 RZ format signal. If the conversion wavelength is given as 1544.0 nm, Fig. 12 shows that Q factor changes with the average power P_1 and P_2 launched into HNLF1 and HNLF2. It can be concluded that the output signal quality can be best with the optimisation of P_1 and P_2. Table 1 lists the optimum P_2 by which the output signal has the best signal quality for different P_1. Figure 13 compares the output eye-diagrams with different power launched into HNLFs, and verifies the optimisation of P_1 and P_2 for the best output signal quality. It is interesting to point out here that, different choice of P_1 and P_2 may have almost the same output signal quality as indicated by Table 1 and the left figures in Fig. 13.

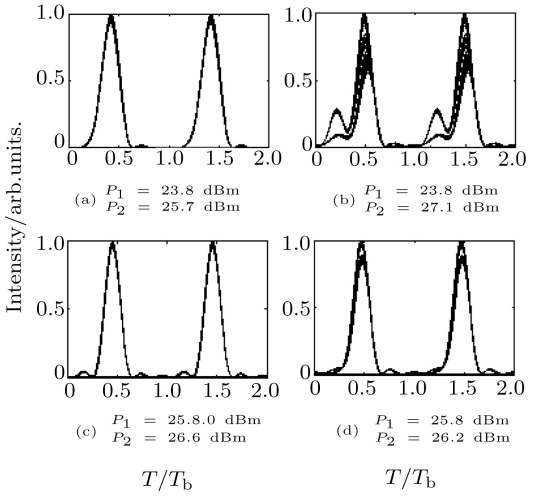


Fig. 13. Output eye-diagrams for different P_1 and P_2.

Table 1. Optimised choice of power launched into HNLFs.

P_1 /dBm	P_2 /dBm	eye-opening	Q /dB
21.8	24.2	0.76	28.0
22.8	24.0	0.90	37.8
23.8	25.9	0.92	38.9
24.8	24.1	0.83	32.0
25.8	24.8	0.93	39.2
25.8	26.6	0.92	38.9
26.8	24.0	0.88	33.2
26.8	27.2	0.87	32.4

9. Conclusions

The impacts of power level launched into HNLFs, conversion wavelength, dispersion slope, modulation format and optical filter bandwidth on the overall performance of optical delay systems are comprehensively studied in this paper. Given the power launched into HNLFs, the time delay generally varies linearly with the conversion wavelength, but jumps intermittently at some conversion wavelengths. It is explained that the seriously distorted signal waveform results in the irregular time delay. The time delay varies semi-periodically with the power launched into HNLFs, and is due to the intra-channel interaction of nonlinearity and dispersion in the fibres. The dispersion slope of HNLFs has significant influence on the time delay, especially for the negative dispersion slope. The time delay differs with modulation formats due to the different combined interaction of nonlinearity and dispersion in fibres. The bandwidth of the optical filters also greatly affects the time delay because it determines the bandwidth of the passed signal in the SPM-based time delay system. The output signal quality of the

overall time delay system depends on the conversion wavelength and input power level, and the optimisation of the power level and conversion wavelength can be made to provide the best output signal quality. The results indicate that the parameters of the SPM-based optical delay system should be deliberately chosen to provide linearly varying time delay and desirable output signal quality. The dependence of the power level and conversion wavelength reveals the limit of convenience to the SPM-based optical delay system, which is also a problem for the cross phase modulation XPM-based optical delay system. Since the SPM and dispersion is transparent to both intensity modulation formats and phase modulation formats, the conclusions in this paper can be similarly extended to the phase modulation formats such as differntial phase shift keying (DPSK).

References

[1] Gauthier D J, Gaeta A L and Boyd R W 2006 *Photon. Spectra* **40** 44

[2] Sakamoto T, Noguchi K, Sato R, Okada A, Sakai Y and Matsuoka M 2001 *Electron. Lett.* **37** 454

[3] Chen C H, Johansson L A, Lal V, Masanovic M L, Blumenthal D J and Coldren L A 2005 *Proc. OFC* OWK4

[4] Ren J, Alic N, Myslivets E, Saperstein R E, McKinstrie C J, Jopson R M, Gnauck A H, Andrekson P A and Radic S 2006 *Proc. ECOC* p1080

[5] Tucker R S, Ku P C and Chang-Hasnain C J 2005 *J. Lightwave Technology* **23** 4046

[6] Zhang B, Yan L S, Zhang L, Nuccio S, Christen L, Wu T and Willner A E 2007 *Proc. ECOC* p944

[7] Mable P Fok and Shu C 2008 *J. Lightwave Technology* **26** 499

[8] Zhang B, Zhang L, Yan L S, Fazal I, Yang J Y and Willner A E 2007 *Opt. Express* **15** 8317

[9] Lenz G, Eggleton B J, Madsen C K and Slusher R E 2001 *J. Quantum Electron.* **37** 525

[10] Christen L, Fazal I, Yilmaz O F, Wu X, Nuccio S, Willner A E, Langrock C and Fejer M M 2008 *Proc. OFC/NFOEC* OTuD1

[11] Okawachi Y, Sharping J E, Xu C and Gaeta A L 2006 *Opt. Express* **14** 12022

[12] Sharping J E, Okawachi Y, Howe J, Xu C, Wang Y, Willner A E and Gaeta A L 2005 *Opt. Express* **13** 7872

[13] Wang Y, Yu C, Yan L, Willner A E, Roussev R, Langrock C, Fejer M M, Sharping J E and Gaeta A L 2007 *Photon. Tech. Lett.* **19** p861

[14] Hu Zh Y and Blumenthal D J 2007 *Proc. OFC* OME4

[15] Agrawal G P 2001 *Nonlinear Fiber Optics* 3rd Ed. (Newyork: Academic) p60, p94